

Supplementary Materials for

Two-dimensional GaSe/MoSe₂ misfit bilayer heterojunctions by van der Waals epitaxy

Xufan Li, Ming-Wei Lin, Junhao Lin, Bing Huang, Alexander A. Puretzy, Cheng Ma, Kai Wang, Wu Zhou, Sokrates T. Pantelides, Miaofang Chi, Ivan Kravchenko, Jason Fowlkes, Christopher M. Rouleau, David B. Geohegan, Kai Xiao

Published 15 April 2016, *Sci. Adv.* **2**, e1501882 (2016)

DOI: 10.1126/sciadv.1501882

This PDF file includes:

- fig. S1. AFM image of MoSe₂ monolayers.
- fig. S2. SEM and AFM images of GaSe/MoSe₂ vdW heterostructures.
- fig. S3. TEM and electron diffraction analyses of the GaSe/MoSe₂ vdW heterostructure.
- fig. S4. Structural analyses of the GaSe/MoSe₂ vdW heterostructure.
- fig. S5. Structure of lateral 1L GaSe/MoSe₂ on the SiO₂/Si substrate.
- fig. S6. Electrical performance of the monolayer GaSe/MoSe₂ lateral junction grown on SiO₂/Si.
- fig. S7. Structural analyses of lateral 1L GaSe/MoSe₂ on 1L MoSe₂.
- fig. S8. AFM image corresponding to the optical image in Fig. 4A.
- fig. S9. Enlarged view of Raman spectra shown in Fig. 4B.
- fig. S10. Calculation of charge transfer between intrinsic GaSe and MoSe₂ monolayers.
- fig. S11. PL emission spectra of MoSe₂ and GaSe/MoSe₂ vdW heterostructures, obtained from PL emission mapping in Fig. 4A.
- fig. S12. Absorption spectra of monolayer GaSe grown on transparent mica.
- fig. S13. DFT calculation of the band structure of the GaSe/MoSe₂ vdW heterostructure.
- fig. S14. I_{ds} - V_{ds} curves under white light illumination across the heterojunction at different back-gate voltages.

Supplementary figures

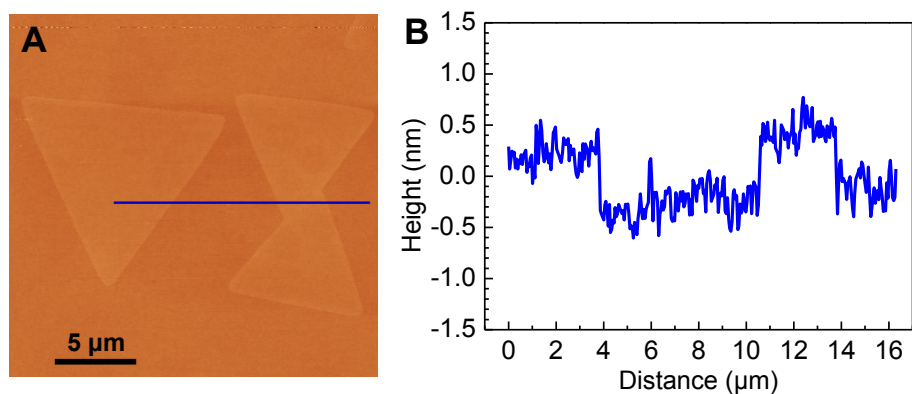


fig. S1. (A) AFM image of 1L MoSe₂ crystals. (B) Height profile along the solid blue line in (A).

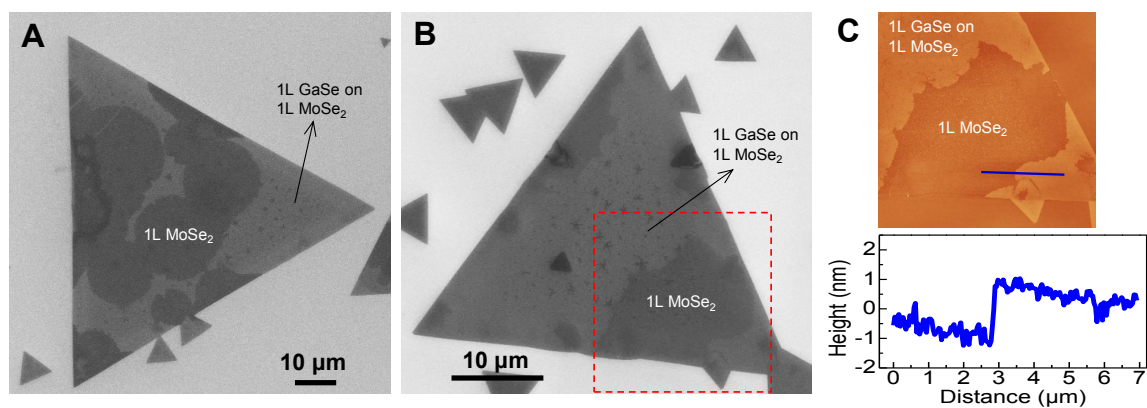


fig. S2. (A and B) SEM images of GaSe/MoSe₂ vdW heterostructures, showing separate, irregularly-shaped 1L GaSe domains formed on 1L MoSe₂. It is noticed that in SEM, the 1L GaSe looks brighter than the underlying 1L MoSe₂. (C) AFM image and height profile (along the solid blue line) corresponding to the area contained by the dashed red square in (B).

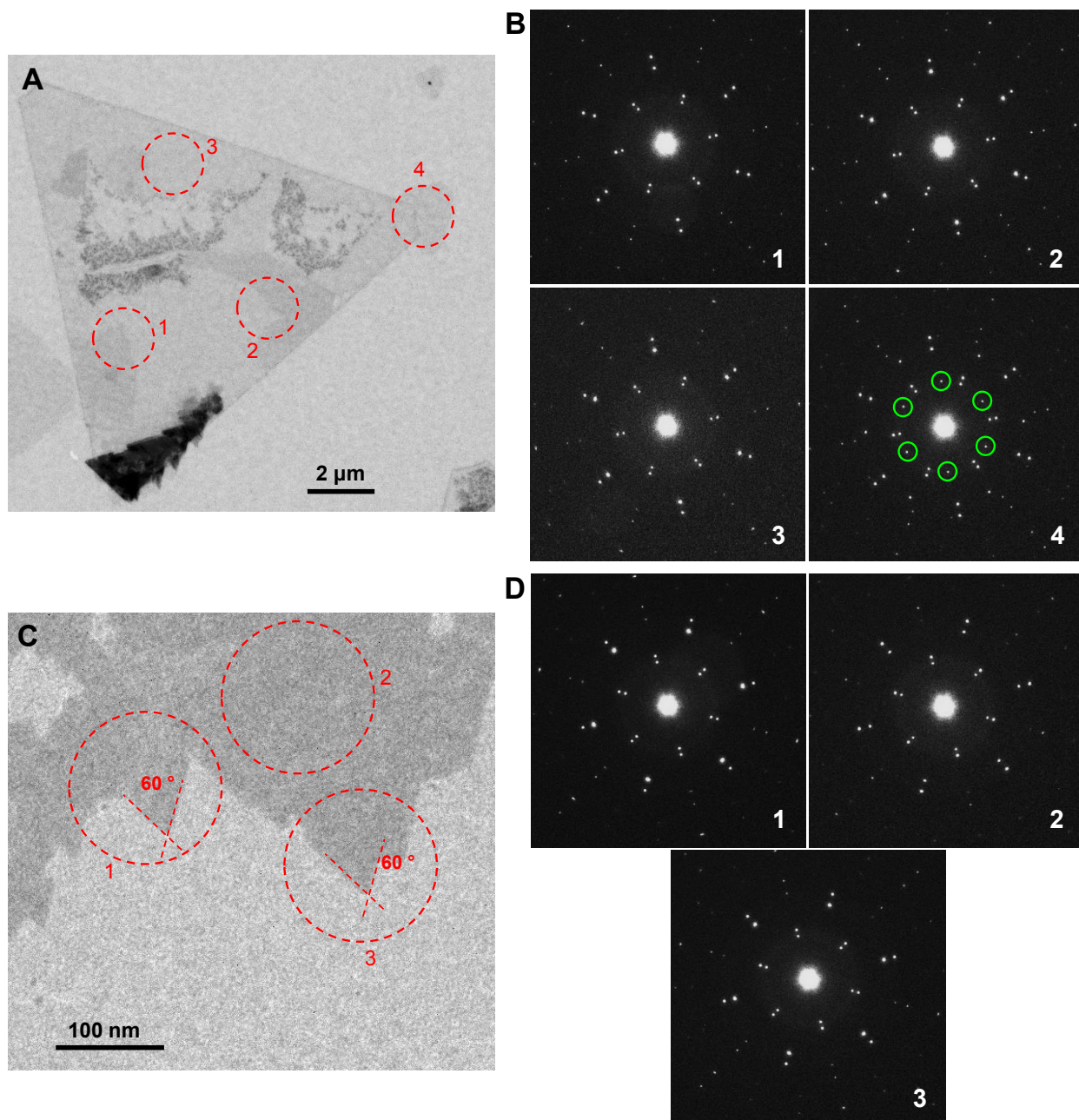


fig. S3. TEM and electron diffraction analyses on GaSe/MoSe₂ vdW heterostructure. (A) Bright-field TEM image of a flake of GaSe/MoSe₂ vdW heterostructure (also with a small domain of GaSe grown laterally as indicated by dashed red circle 4) (B) Electron diffraction patterns 1, 2, 3, and 4 obtained from areas contained by dashed red circle 1, 2, 3, and 4 in (A). The diffraction patterns show that in the GaSe/MoSe₂ vdW heterostructure, the lattice of GaSe and MoSe₂ are

well aligned at the same orientation, while in pattern 4, the circled spots come from the lattice of GaSe domain grown laterally, which always rotates from that of MoSe₂. (C) Bright-field TEM image showing edge area of a monolayer vdW epitaxial GaSe domain on MoSe₂. (D) Electron diffraction patterns 1, 2, and 3 obtained from areas contained by dashed red circle 1, 2, and 3 in (C). The diffraction patterns indicate that the GaSe domain at the edge have the same lattice orientation as the inner regions.

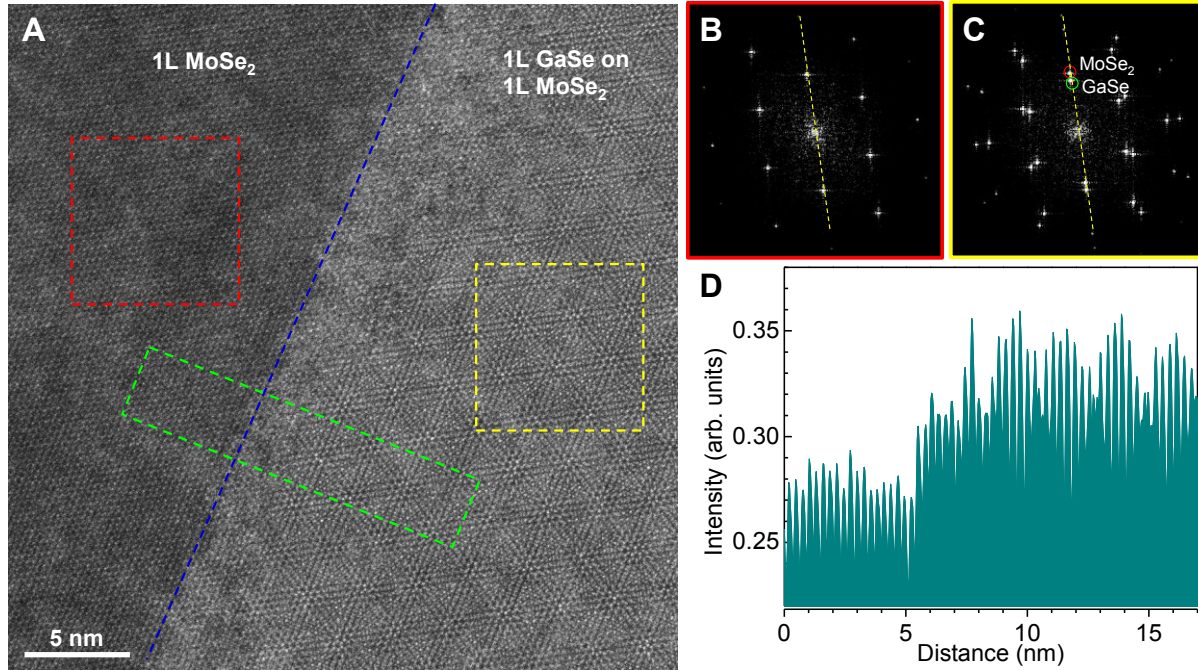


fig. S4. Structural analyses of the GaSe/MoSe₂ vdW heterostructure. (A) Top-view atomic resolution Z-contrast STEM image showing the edge area of GaSe domain on MoSe₂. The dashed blue line indicates the edge of GaSe domain. The region at the left side of the dashed blue line shows typical honeycomb atomic structure of 1L MoSe₂, with a lattice constant $a = 0.329$ nm. The region at the right side of the dashed blue line shows a Moiré pattern the same as that shown in Fig. 2B, indicating a periodic superlattice with lattice constant $L = 2.63$ nm formed by 1L GaSe stacked on 1L MoSe₂. (B and C) FFT images acquired from the region contained by the dashed red (B) and yellow (C) squares, respectively, in (A). (B) shows a hexagonal diffraction pattern from 1L MoSe₂, while (C) exhibits two sets of hexagonal diffraction patterns from 1L MoSe₂ and 1L GaSe with well-aligned registry, demonstrating that the growth of GaSe domains was controlled by the underlying MoSe₂ *via* vdW epitaxy. (D) Intensity profiles along the dashed green rectangle from the left to right in (A).

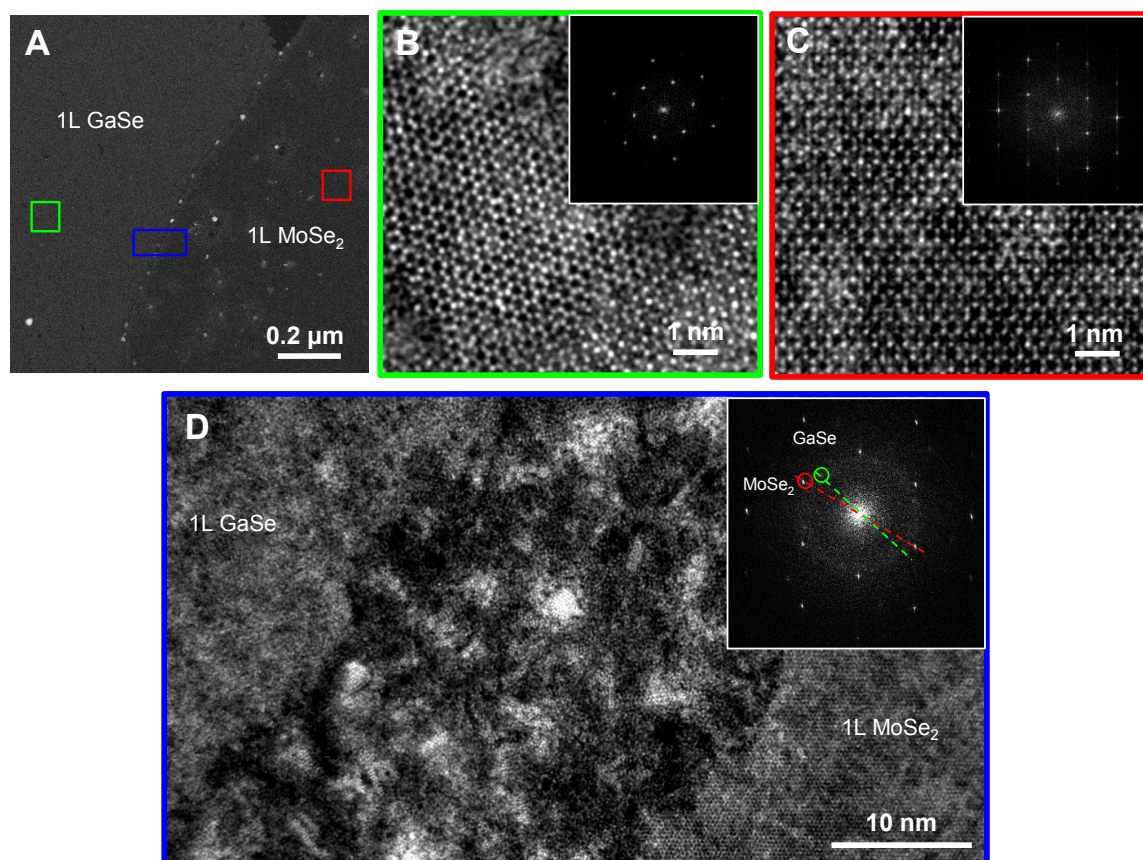


fig. S5. Structure of lateral 1L GaSe/MoSe₂ on SiO₂/Si substrate. (A) Dark-field STEM image of 1L GaSe domain grown laterally from 1L MoSe₂. (B–D) Top-view atomic resolution Z-contrast STEM images from the areas contained by the solid green, red, and blue squares in (A), corresponding to 1L GaSe, 1L MoSe₂, and the region near the GaSe/MoSe₂ boundary, respectively. Insets are FFT images. These images show that the two lattices are not aligned and always show an arbitrary rotation angle with respect to each other, and there is no clear grain boundary between the two crystals, indicating that the laterally grown GaSe has no epitaxial relationship with MoSe₂.

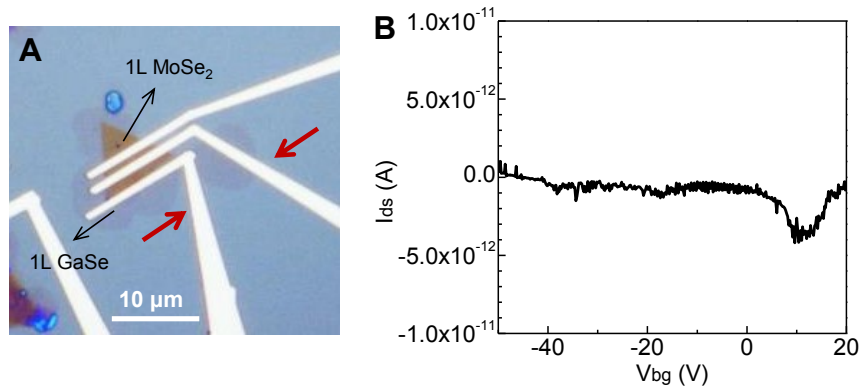


fig. S6. (A) Optical micrograph of a FET device made on a monolayer lateral GaSe/MoSe₂ junction on SiO₂/Si, and used for measuring the electrical properties across the junction. The measurement was conducted using the electrodes indicated by the solid red arrows. (B) Transfer curve of the monolayer lateral GaSe/MoSe₂ junction in (A). However, the current can hardly be detected across the junction of this lateral GaSe/MoSe₂ junction due to the disordered region at the boundary between GaSe and MoSe₂ as shown in Fig. S5.

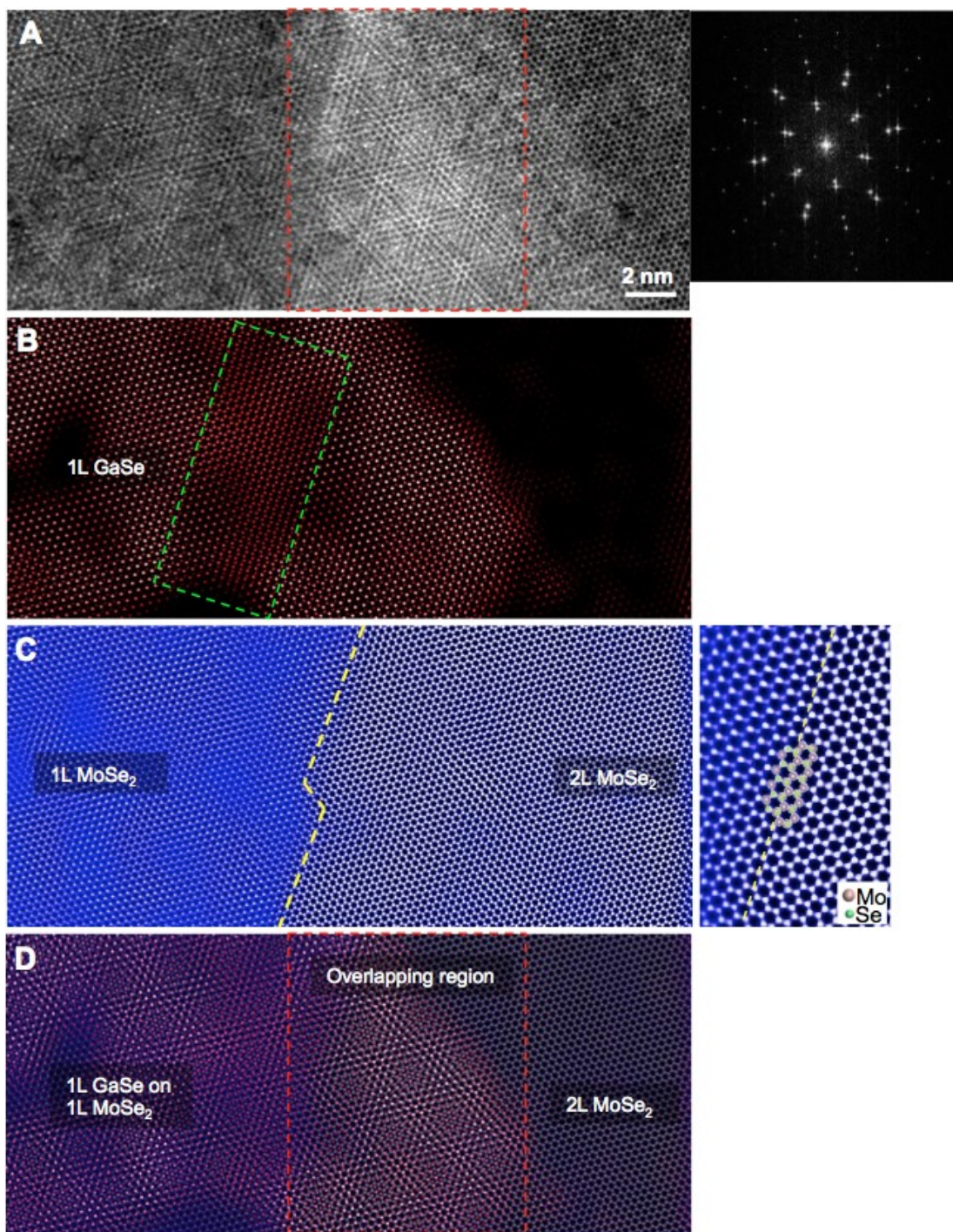


fig. S7. Structural analyses of lateral 1L GaSe/MoSe₂ on 1L MoSe₂. **(A)** Top-view atomic resolution Z-contrast STEM image showing an overlap region (as indicated by the dashed red rectangle) of the lateral 1L GaSe domain and second layer of MoSe₂, which is the same as Figure 3A, and FFT image. **(B)** Inverse FFT image of 1L GaSe. The dashed green rectangle highlights the inclined region of the monolayer layer GaSe where the lattice spacing has changed. **(C)**

Inverse FFT image of 1L and 2L MoSe₂. The yellow dashed line highlights the step edge of the 2L MoSe₂. The image beside is the enlarged view of edge area, showing that the second MoSe₂ layer has a Se-terminated zigzag edge. **(D)** Overlapped inverse FFT images in **(B)** and **(C)**.

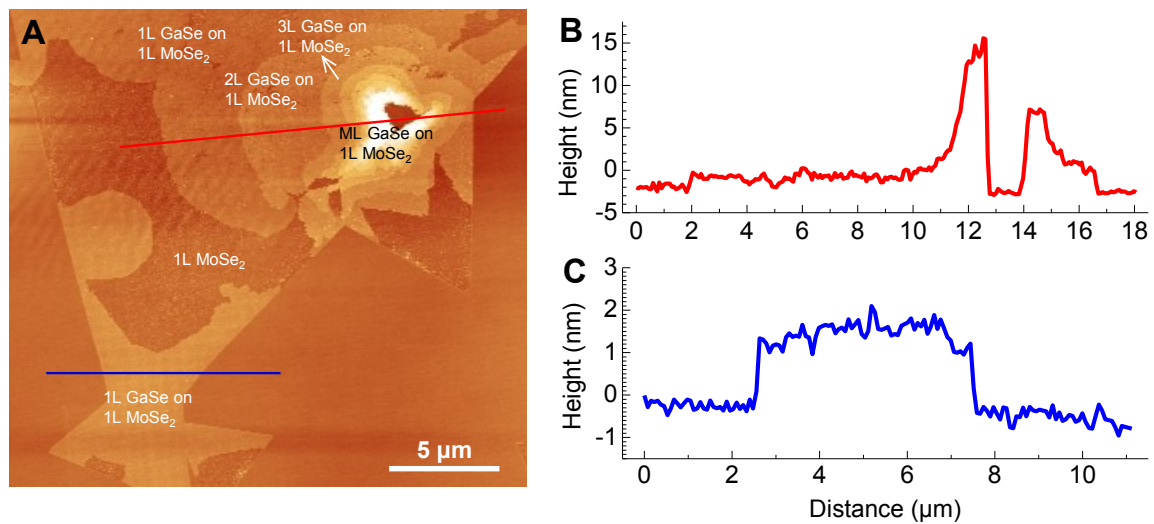


fig. S8. **(A)** AFM image corresponding to the optical image in Fig. 4A. **(B and C)** Height profiles along the solid red and blue lines in **(A)**, respectively.

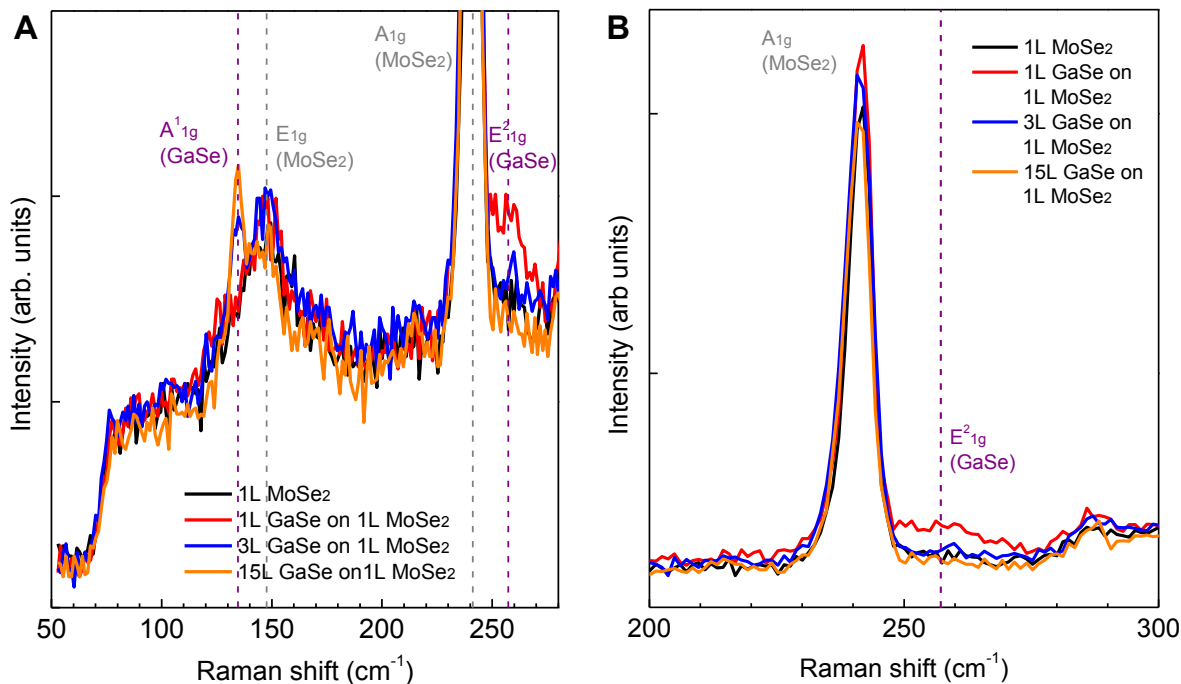


fig. S9. (A and B) Enlarged view of Raman spectra shown in Fig. 4B, showing the decrease of the GaSe A^1_{1g} mode as the thickness decreases, and the enhancement of E^2_{1g} vibration mode of 1L GaSe on 1L MoSe₂.

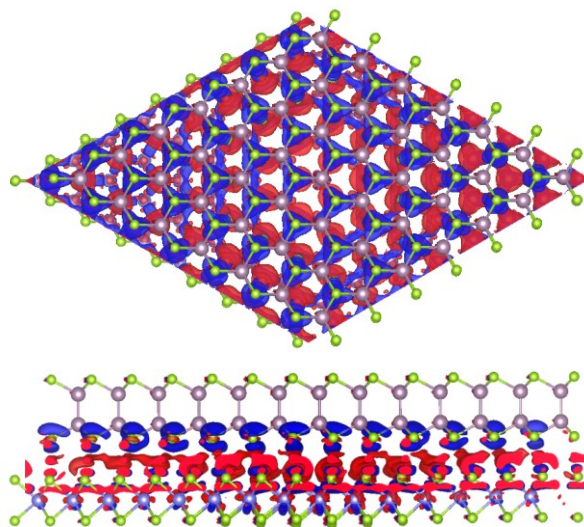


fig. S10. Calculation of charge transfer between intrinsic 1L GaSe and MoSe₂ (Top: top-view; Bottom: side-view), which is 0.2e (per supercell). Note that blue means loss of electrons while shown in red means gain of electrons.

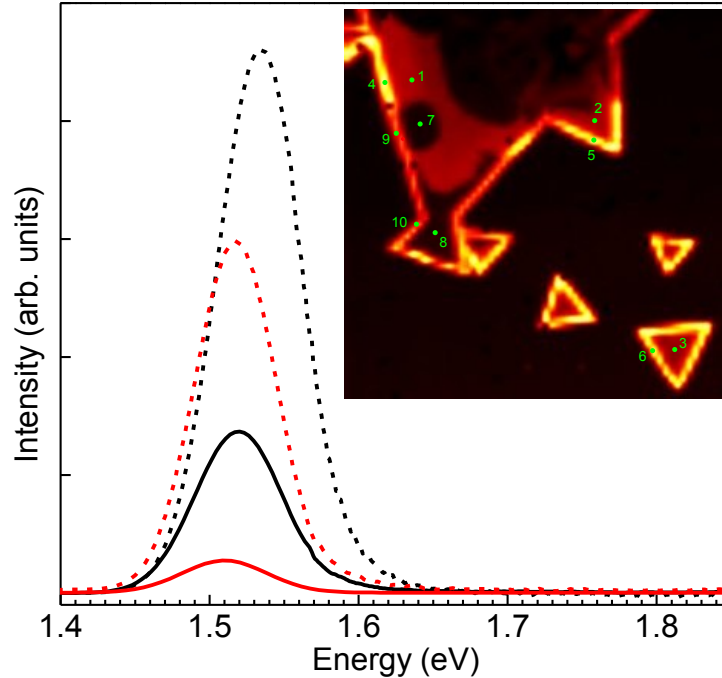


fig. S11. PL emission spectra of MoSe₂ and GaSe/MoSe₂ vdW heterostructures obtained from PL emission mapping in the inset (Fig. 4A). Solid black curve corresponds to the inner region of pure 1L MoSe₂ (spots 1, 2, and 3), dashed black curve corresponds to the edge of 1L MoSe₂ (spots 4, 5, and 6), solid red curve corresponds to the inner region of 1L GaSe/1L MoSe₂ vdW heterostructure (spots 7 and 8), and dashed red curve corresponds to the edge of 1L GaSe/1L MoSe₂ vdW heterostructure (spots 9 and 10). The emission intensities decrease dramatically in the regions with GaSe layers compared to those with bare 1L MoSe₂, and the edge shows enhanced PL when compared to inner region. The enhancement of emission intensity at edge is also accompanied by blue-shifted emission bands, which are observed on edges with and without GaSe layers. Therefore, we believe the enhanced and blue-shifted emission at edge is not due to the growth of GaSe layers, but may be caused by several possible factors including dielectric environment, strain, adsorbates/clusters, and defects.

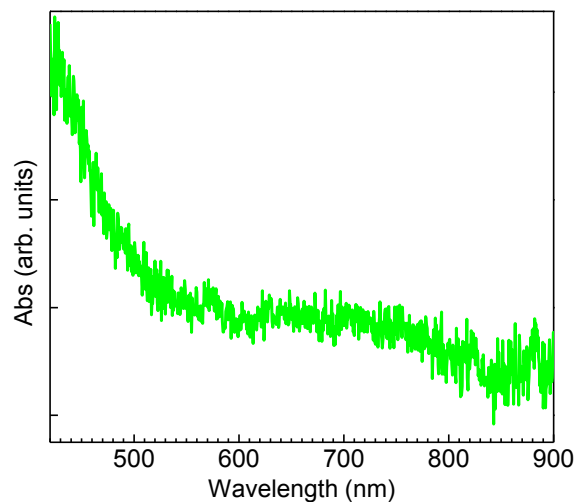


fig. S12. Absorption spectra of monolayer GaSe grown on transparent mica. No obvious absorption band is observed, indicating the indirect bandgap of monolayer GaSe, which is in agreement with our previous calculation (see ref 4 in the main text).

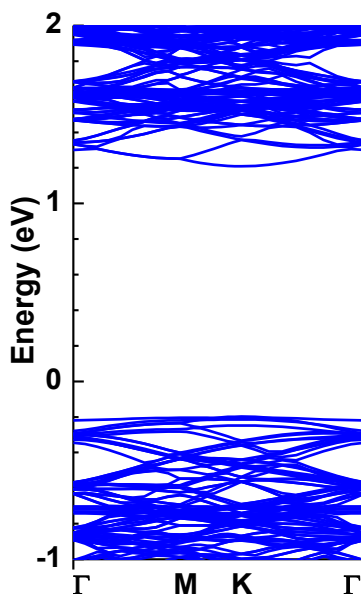


fig. S13. DFT calculation of the band structure of the GaSe/MoSe₂ vdW heterostructure. The band structure generally maintains that of monolayer MoSe₂, but shows more states and a flatter valence band maximum (VBM) due to the contribution from GaSe.

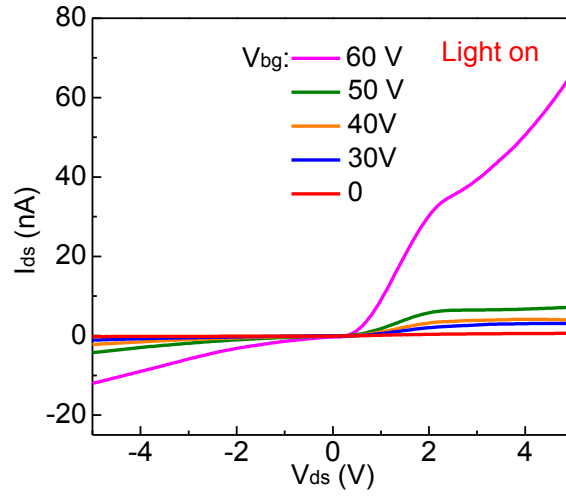


fig. S14. I_{ds} - V_{ds} curves across the heterojunction at different back-gate voltages and under white light illumination.